Unusual Thermal Properties of Certain Poly(3,5-disubstituted styrenes)

Journal:	*Macromolecules*
Manuscript ID	ma-2020-00163q.R1
Manuscript Type:	Article
Date Submitted by the Author:	08-May-2020
Complete List of Authors:	Koh, Jai Hyun; University of Texas at Austin, McKetta Department of Chemical Engineering Zhu, Qingjun; University of Texas at Austin, Chemical Engineering Asano, Yusuke; The University of Texas, Department of Chemistry Maher, Michael; University of Minnesota Twin Cities, Ha, Heonjoo; University of Minnesota Twin Cities, Chemical Engineering and Materials Science Kim, Sung-Soo; University of Minnesota Twin Cities, Chemical Engineering and Materials Science Cater, Henry; University of Texas at Austin, Chemistry Mapesa, Emmanuel; University of Tennessee, Chemical and Biomolecular Engineering Sangoro, Joshua; University of Tennessee Knoxville, Department of Chemical and Biomolecular Engineering Ellison, Christopher; University of Minnesota Twin Cities, Chemical Engineering and Materials Science Lynd, Nathaniel; University of Texas at Austin, McKetta Department of Chemical Engineering Willson, C.; University of Texas at Austin, Chemical Engineering;

Unusual Thermal Properties of Certain Poly(3,5-disubstituted styrenes)

Jai Hyun Koh,[†,‡] Qingjun Zhu,[†,‡] Yusuke Asano,[‡] Michael J. Maher,[∥] Heonjoo Ha,[∥]

Sung-Soo Kim,[∥] Henry L. Cater,[§] Emmanuel U. Mapesa,[⊥] Joshua R. Sangoro,[⊥]

Christopher J. Ellison,[∥] Nathaniel A. Lynd,[‡] and C. Grant Willson[*,‡,§]*

[†]These authors contributed equally to this work.

[‡]McKetta Department of Chemical Engineering and [§]Department of Chemistry, The University of Texas at Austin, Austin, Texas 78712, United States

[⊥]Department of Chemical and Biomolecular Engineering, University of Tennessee, Knoxville, Tennessee 37996, United States

[∥]Department of Chemical Engineering and Materials Science, University of Minnesota, Minneapolis, Minnesota 55455, United States

Corresponding Authors

*Email: willson@che.utexas.edu (C.G.W.)

ABSTRACT: During the course of studying silicon-containing diblock copolymers, it was discovered that poly(3,5-di(trimethylsilyl)styrene)-*block*-poly(3,4-methylenedioxystyrene) (PDTMSS-*b*-PMDOS) showed very unusual thermal properties. The material can be recovered as a free-flowing powder after heating above 250 °C. To better understand this behavior, homopolymers of the 3,5-disubstituted styrenes, poly(3,5-di(trimethylsilyl)styrene) (PDTMSS) and poly(3,5-di-*tert*-butylstyrene) (PDtBS), were prepared. These polymers are soluble in common organic solvents and form clear, glassy thin films upon spin coating. These homopolymers were studied by differential scanning calorimetry (DSC), broadband dielectric spectroscopy (BDS), dynamic mechanical analysis (DMA), and temperature-programmed ellipsometry. These experiments document the lack of a conventional glass transition in these materials below their decomposition temperature. A series of statistical copolymers of PDTMSS and PDtBS with styrene was synthesized and studied by DSC in attempt to establish the T_g of the homopolymers by model-based extrapolation.

Introduction

Block copolymers (BCPs) are of great interest in the lithographic patterning field due to their propensity to phase separate into regular microdomains with sizes on the length scale of three to several hundred nanometers.[1] This is exactly the dimensional regime of the structures that must be generated in order to produce the next generations of microelectronic devices. Production of such devices demands the use of these materials in thin films and requires that one of the blocks in the copolymer can be selectively removed to provide patterned access to the substrate. Diblock copolymers in which one block incorporates a significant mole fraction of silicon are particularly attractive materials for this end use. This is because the other block without silicon can be selectively removed by reactive ion etching, while the block with silicon has high etch resistance and remains after etching.[2,3] This high etch selectivity between the two blocks gives sufficient etch contrast for subsequent pattern transfer into functional substrates. A number of such silicon-containing BCPs have been reported together with detailed demonstrations of their performance and promise. These include polystyrene-*block*-polydimethylsiloxane,[4–6] polydimethylsiloxane-*block*-polylactide,[7,8] polydimethylsiloxane-*block*-poly(methyl methacrylate),[9] polylactide-*block*-polydimethylsiloxane-*block*-polylactide,[10] polystyrene-*block*-poly(4-trimethylsilylstyrene)-*block*-polystyrene,[11,12] polystyrene-*block*-poly(4-trimethylsilylstyrene),[13–15] polystyrene-*block*-poly(4-pentamethyldisilylstyrene),[14] poly(4-methoxystyrene)-*block*-poly(4-trimethylsilylstyrene),[14,16] poly(4-methoxystyrene)-*block*-poly(4-pentamethyldisilylstyrene),[17] poly(4-trimethylsilylstyrene)-*block*-polylactide,[11,18] polystyrene-*block*-polytrimethylsilylisoprene,[19] and poly(3,4-methylenedioxystyrene)-*block*-poly(4-pentamethyldisilylstyrene).[20]

In the course of efforts to develop the knowledge required to design improved silicon-containing BCPs for this sort of application, many analogs were synthesized and characterized.

One of these materials, poly(3,5-di(trimethylsilyl)styrene)-*block*-poly(3,4-methylenedioxystyrene) (PDTMSS-*b*-PMDOS) (**Scheme 1**) showed very unusual properties. In particular, it was not possible to document the morphology of this BCP because, unlike other mono-substituted styrene-based polymer analogs, it could not be thermally annealed below its decomposition temperature. Thermal annealing is required to refine the domain ordering of BCP thin films after spin casting in the course of forming them into etch masks. Solvent vapor annealing can also be used for this purpose but is unattractive to end users for a variety of reasons. Remarkably, after heating PDTMSS-*b*-PMDOS to temperatures well in excess of 180 °C, the polymer was still a free-flowing powder.

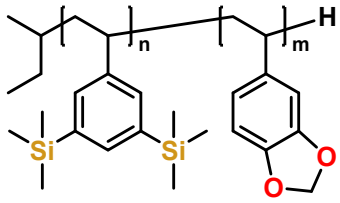

Scheme 1. Chemical structure of PDTMSS-*b*-PMDOS which could not be thermally annealed below its decomposition temperature.

Another silicon-containing BCP that includes the PMDOS block, poly(3,4-methylenedioxystyrene)-*block*-poly(4-pentamethyldisilylstyrene) (PMDOS-*b*-PDSS), has been fully characterized and reported. It does not exhibit this unusual thermal behavior.[20,21] This led to the hypothesis that the glass transition temperature (T_g) of this particular silicon-containing block, PDTMSS, is unusually high. To more closely examine this behavior, the PDTMSS homopolymer was prepared by free radical polymerization and fully characterized. It is a soluble, unremarkable polymer except that no T_g can be detected by differential scanning calorimetry (DSC). Even modulated DSC characterization, that offers high resolution and sensitivity and is often used to detect very small phase transitions of liquid crystals, showed no detectable T_g for the PDTMSS

homopolymer. No distinct evidence of a transition could be recorded and the samples remained powdery after heating above 250 °C.

Curiosity demanded some rationalization for this unusual behavior. So, a series of homopolymers of different 3,5-disubstituted styrene monomers were synthesized or purchased and subjected to DSC characterization. Some pertinent analogs and their corresponding T_gs are listed in **Figure S1**. The change from 3,5-dimethyl and 3,5-diisopropyl to 3,5-di-*tert*-butyl is very interesting. Poly(3,5-di-*tert*-butylstyrene) (PDtBS) displays all of the thermal characteristics that were observed from studies of the 3,5-di(trimethylsilyl) analog. The unusual behavior of the PDtBS and PDTMSS homopolymers inspired an attempt to document the T_gs of these materials by other analytical methods.

The T_g of multi-substituted styrene containing polymers is generally higher than that of PS.[22,23] This trend has generally been ascribed to the added chain backbone rigidity caused by the ring substituents. This added rigidity in turn restricts cooperative segmental mobility (*i.e.*, backbone chain mobility associated with alpha-relaxation processes and T_g). The reported T_gs rarely exceed 200 °C. An interesting exception is copolymers of 4-chlorostyrene and [4-tris(trimethylsilyl)methyl]methylstyrene, which are reported to have T_g in excess of 250 °C.[24]

Results and Discussion

Figure 1a shows the DSC traces of the PDTMSS, PDtBS, and poly(4-trimethylsilylstyrene) (PTMSS) homopolymers. The polymers were heated to 200 °C at a heating rate of 10 °C/min. The PTMSS trace shows very significant heat flow and is provided for a comparison. However, no T_g was observed for both PDTMSS and PDtBS samples. Alternatively, *in-situ* ellipsometry was used to record the thickness of thin films of these polymers as a function of temperature in the hope of finding the change in slope (change in coefficient of thermal expansion) that is characteristic of

the T_g of a polymer.[25] *In-situ* ellipsometry measurements were performed for PDTMSS and PDtBS films on silicon wafers. The T_gs of polymer thin films can be dependent on film thickness. For polymers like these which lack significant interactions (*e.g.*, hydrogen bonding, *etc.*) with the native oxide on silicon wafers, T_g typically decreases with decreasing film thickness, mostly due to enhanced cooperative segmental mobility afforded by the air-film interface.[26] For example, when the film thickness of PS is greater than 100 nm, the T_g is the same as that of bulk PS but it decreases precipitously for film thicknesses below 100 nm.[27] Because the T_gs of bulk PDTMSS and PDtBS homopolymers cannot be determined using DSC, attempts were made to determine the T_gs of homopolymer thin films using *in-situ* ellipsometry. Film thicknesses greater than 200 nm were used to minimize any influence from film thickness on T_g. In order to validate the experimental setup for *in-situ* ellipsometry, the thickness of a PS homopolymer film on silicon wafer was measured as a function of temperature as shown in **Figure S2**.

Below 80 °C, PS is in the glassy state and shows a linear dependence of the film thickness on temperature. At temperatures higher than 110 °C, PS is in the melt state and again shows a linear dependence on temperature albeit with a steeper slope. In the temperature region between 80 °C and 110 °C, the sample thickness showed a nonlinear dependence on temperature. This region corresponds to the glass transition region of PS. The T_g of the PS thin film with an initial thickness of *ca.* 200 nm was determined by fitting the data to **eq 1**.[25]

$$h(T) = w\left(\frac{M-G}{2}\right)\ln\left[\cosh\left(\frac{T-T_g}{w}\right)\right] + (T-T_g)\left(\frac{M+G}{2}\right) + c \quad (1)$$

Here the film thickness (h) is expressed as a function of temperature (T), w is the width of the transition between the melt and glass states, c is the film thickness at $T = T_g$, and the variables G and M are the dh/dT slopes for the glass and melt states, respectively. To prevent multiple

solutions, the upper bound of w was kept at 35 °C during the fitting. The T_g of the PS film based on this fitting was 97 °C, which is consistent with the bulk T_g (99 °C) as determined by DSC. After this validation, PDTMSS and PDtBS films with initial film thicknesses of 306 nm and 339 nm, respectively, were subjected to the same *in-situ* ellipsometry measurement. The plots of the measured film thickness versus temperature are shown in **Figure 1b,c**. Unlike the PS film, there are no distinct regions of different slopes on either plot. On the contrary, an exponential increase in film thickness with increasing temperature was observed for both of them. This may indicate that the polymer films did not undergo a glass transition especially considering that both bulk polymers remained powdery after corresponding DSC measurements. **Eq 1** is valid for any measurement that shows linear dependence of the film thickness on temperature in the melt and the glass regions. However, using the upper bound of 35 °C for w and allowing c, T_g, G, and M to vary gave the fits depicted in **Figure 1b,c** and **Table S1**. This analysis gave T_gs of 91 °C and 135 °C for PDTMSS and PDtBS, respectively. These estimated T_g values are clearly not reliable since no evidence of a glass transition occurred at either of these two temperatures in the DSC measurements and the samples were free-flowing powders after heating well above these temperatures.

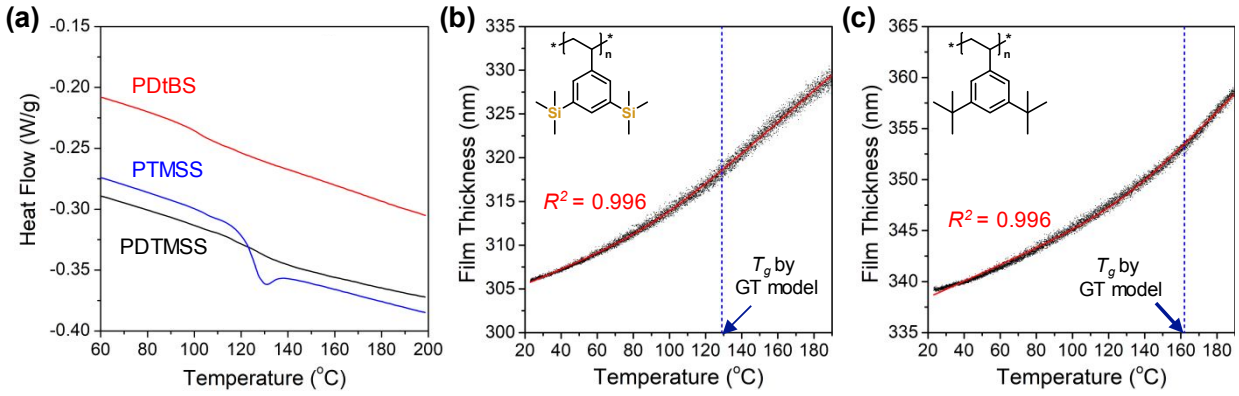

Figure 1. (a) DSC traces for PDTMSS, PDtBS, and PTMSS homopolymers at a heating rate of 10 °C/min. (b,c) *In-situ* ellipsometry measurements of thin films of (b) PDTMSS and (c) PDtBS homopolymers. The T_g of each homopolymer estimated by Gordon–Taylor (GT) model was shown by blue dotted lines.[28]

The decomposition temperatures of PDTMSS and PDtBS homopolymers were then measured by TGA (**Figure S3a**). The homopolymers have very similar decomposition temperatures, which start at around 275 °C. The homopolymers were also studied using an SRS Optimelt melting point apparatus as shown in **Figure S3b.** PS homopolymer was used as a control. PS showed the sharp decrease in reflected light intensity at around 100 °C. This temperature was consistent with the T_g of PS, which was determined to be 99 °C by the DSC measurement. No significant changes of the reflected light intensity were observed when heating PDTMSS and PDtBS homopolymers until around 275 °C. Above 275 °C, a dramatic decrease of intensity was observed, which is attributed to the decomposition of the homopolymers based on the TGA results. This confirms that the PDTMSS and PDtBS homopolymers start to decompose (lose mass) at around 275 °C, but no change in reflected light intensity was observed at lower temperatures.

The PDTMSS and PDtBS homopolymers were also characterized by broadband dielectric spectroscopy (BDS) in an attempt to determine their dynamic T_gs. Sample capacitors made by coating thin polymer films on n-type As-doped silicon wafers (resistivity: 1–5 mΩ • cm, thickness:

500 ± 10 µm, orientation: <100> ± 0.5°) were assembled using a nanostructured electrode arrangement, where a regular matrix of highly insulating silica nanostructures served as spacers. Detailed information about the use of this capacitor arrangement can be found elsewhere.[29–31] A layer of silver paint was applied on the back side of the silicon wafers to improve electrical contact.

Figure S4 shows the dielectric loss as a function of frequency for a set of temperatures in the range of 250–500 K. At low temperatures (250 and 280 K), a fairly well-resolved dielectric relaxation was observed that can be described by the empirical Havriliak-Negami (HN) function (**eq 2**, see dashed lines in **Figure S4a**):

$$\varepsilon^* = \varepsilon_\infty + \frac{\Delta\varepsilon}{[1+(i\omega\tau_{HN})^\beta]^\gamma} \quad (2)$$

where $\omega = 2\pi f$, ε_∞ is the high-frequency of the dielectric permittivity, $\Delta\varepsilon$ is the dielectric relaxation strength, τ_{HN} is the relaxation time, and β and γ are shape parameters.[32] At higher temperatures above ~360 K, another relaxation process is evident, albeit obscured by low-frequency dispersion due to the contribution of d.c. ionic conductivity. To characterize this process, the derivative analysis (an approach popularized by Wübbenhorst and van Turnhout) where the dielectric loss is approximated as $\varepsilon''_{der} = (-\pi/2)\partial\varepsilon'/\partial\ln(f)$ was used.[33] This representation suppresses the contribution of ionic d.c. conductivity to the dielectric loss and enables access to relaxations that are otherwise not readily evident in the raw dielectric spectra. For graphical clarity, **Figure S4c** shows the spectra obtained by applying this approach. As an illustration, the spectrum measured at 490 K is fitted to a modified HN function that includes an extra term, $-i(\sigma_0 / \varepsilon_0\omega^s)$, to account for the low-frequency flank (*i.e.* d.c. conductivity modeled by the dotted line). Here, σ_0 is the d.c. conductivity of the sample, ε_0 is the dielectric permittivity of free space, and $s \leq 1$ is a scaling

parameter, whose value depends on the origin of the conductivity. The mean molecular relaxation times (τ) associated with the two processes were calculated from the fit parameters of **eq 3**

$$\tau = \tau_{HN} \sin\left(\frac{\beta\gamma\pi}{2+2\gamma}\right)^{1/\beta} \sin\left(\frac{\beta\pi}{2+2\gamma}\right)^{-1/\beta} \quad (3)$$

and are plotted as functions of inverse temperature in **Figure S4d**. The low-temperature process exhibits an Arrhenius-type temperature dependence, which is characteristic of secondary or localized relaxations, as given by **eq 4**:

$$\tau(T) = \tau_{\infty} \exp\left(-\frac{E_a}{k_B T}\right) \quad (4)$$

Here, E_a denotes the activation energy, k_B is the Boltzmann constant, and τ_∞ is the mean relaxation time in the high temperature limit. Fitting this process by **eq 4** delivers an activation energy of 21.8 ± 0.1 kJ/mol. This magnitude of E_a is consistent with libration motion of the benzene ring.[34] The high-temperature process exhibits a non-Arrhenius temperature dependence and can be approximated by the empirical Vogel-Fulcher-Tammann (VFT) equation (**eq 5**):

$$\frac{1}{\tau(T)} = \frac{1}{\tau_{\infty}} \exp\left(-\frac{DT_V}{T - T_V}\right) \quad (5)$$

where D is a material-dependent constant and T_V denotes the Vogel temperature (*i.e.* ideal T_g). At the calorimetric T_g, $\tau(T_g)$ reaches a typical value of ~100 s (and a viscosity of ~10^{13} poise) for most materials, hence a dielectrically-determined T_g can be obtained.[35] Using this convention, a T_g of 127 ± 2 °C is reported for PDtBS homopolymer, which is not consistent with the DSC or ellipsometry measurements. The rather high values of τ_∞ obtained from the VFT fits indicate that this relaxation is likely of interfacial origin, arising from internal interfaces within the powdery samples rather than segmental dynamics. The data for the PDTMSS sample (**Figure S4b**) were

quite noisy since the dielectric loss values (< 10^{-4}) are at the limit of the dielectric spectrometer. This is presumably due to the nearly zero dipole moment of the DTMSS moiety. Detailed analysis of these data was limited by the low signal levels, although there seem to be two dielectric relaxations present in the PDTMSS as well. Thus, T_g of the PDTMSS homopolymer cannot be obtained from the BDS spectra. This observation is unexpected since the localized relaxations determined from BDS data suggest that the dipole moments corresponding to motions of sub-moieties are detectable and should ultimately contribute to segmental dynamics, which would determine the T_g. Given the absence of measurable segmental relaxations from the BDS spectra, it is likely that the polymers investigated adopt preferred conformations of neighboring chains that result in cancellation of the effective dipole moments. Such molecular arrangements would explain the presence of secondary relaxations and lack of T_gs in the polymers studied. An alternative hypothesis is that the bulky nature of the monomers impedes segmental motion in these systems. By combining BDS results with those from the other techniques, we argue in this work that the latter hypothesis is more probable.

Dynamic mechanical analysis (DMA) was also performed to determine the T_g of the PDtBS homopolymer as illustrated in **Figure S5**. The PDtBS sample was solution cast from toluene, dried at room temperature for two weeks and then heated in a vacuum oven at 160 °C for 24 h prior to the measurement. First, the sample was subjected to DMA analysis at fixed temperatures of 25, 100, and 200 °C. Then, another set of storage modulus measurements was made during a temperature sweep from 100 °C to 230 °C. The data were reproducible and clearly show a transition behavior around 170 °C. However, it is not clear that this is a T_g since the modulus change across it was relatively small compared to a typical T_g and the material remained solid with a relatively high modulus above 10^7 Pa at the end of the measurement at 230 °C. The transition is

more likely attributable to localized dynamic modes rather than segmental relaxation associated with T_g.

In principle, it should be possible to create a statistical copolymer of either DTMSS or DtBS and styrene that has an accessible T_g since the T_g of the PS homopolymer is around 100 °C. The T_g of the statistical copolymer block could, again in principle, be tuned to any temperature between the T_gs of homopolymers made of the two constituent monomers. In addition, synthesis of such statistical copolymers and measurement of their T_gs as a function of composition would allow extrapolation to the T_g of the homopolymer (PDTMSS or PDtBS). That extrapolated value could be insightful. Therefore, an effort was initiated to make a series of such copolymers.

The integrated copolymer equation established by Meyer and Lowry was used to determine the reactivity ratios between styrene (S) and 3,5-disubstituted styrene (DTMSS or DtBS).[36] The Meyer–Lowry equation is shown in **eq 6**:

$$\text{Conversion} = 1 - \left(\frac{f_A}{f_A^0}\right)^{\frac{r_B}{1-r_B}} \left(\frac{1-f_A}{1-f_A^0}\right)^{\frac{r_A}{1-r_A}} \left(\frac{f_A(2-r_A-r_B)+r_B-1}{f_A^0(2-r_A-r_B)+r_B-1}\right)^{\frac{r_A r_B-1}{(1-r_A)(1-r_B)}} \quad (6)$$

where total conversion of both monomers is expressed as a function of the molar fraction of monomer A (f_A) at any given reaction time, f_A^0 is the initial molar fraction, r_A and r_B are reactivity ratios for monomer A and monomer B, respectively. The total conversion of both monomers is calculated using **eq 7**:

$$\text{Conversion} = 1 - \frac{[A]+[B]}{[A]_0+[B]_0} \quad (7)$$

where $[A]$ and $[B]$ are the concentrations of monomer A and monomer B at any given reaction time, and $[A]_0$ and $[B]_0$ are initial concentrations of monomer A and monomer B before the polymerization.

^{1}H NMR spectroscopy can be used to monitor the composition of monomers and the total conversion during a copolymerization process by integration of distinguishable proton peaks from each monomer.[37,38] The free radical copolymerization of DTMSS and styrene (S) was carried out in an NMR tube in a 600 MHz spectrometer, and ^{1}H NMR spectra were acquired every hour for 11 h as shown in **Figure S6**. The monomer concentration, [DTMSS] or [S], was monitored using a relative integral (A_{DTMSS} or A_S) of the proton peaks from each monomer normalized by the total integral of all the peaks present in the spectrum. The spectrum (**Figure S6**) shows two distinguishable peaks, that at 5.71 ppm (1H) from DTMSS shaded in yellow and that at 5.56 ppm (1H) from styrene, shaded in blue, that were used in this analysis. The molar fraction of DTMSS monomer at any time during the copolymerization was calculated using **eq 8**. The total conversion of both monomers was calculated using **eq 9**.

$$f_{DTMSS} = \frac{A_{DTMSS}}{A_{DTMSS} + A_S} \tag{8}$$

$$\text{Conversion} = 1 - \frac{A_{DTMSS} + A_S}{A_{DTMSS,0} + A_{S,0}} \tag{9}$$

The copolymerization kinetics data for DTMSS and styrene are summarized in **Table S2**. The plot of the total conversion versus the molar fraction of DTMSS (f_{DTMSS}) is shown in **Figure 2a**. Fitting these data with the Meyer–Lowry equation provided the reactivity ratios of DTMSS and styrene as $r_{DTMSS} = 0.6 \pm 0.1$ and $r_S = 0.9 \pm 0.1$, respectively. The monomer composition ratio barely changed during the copolymerization, indicating that the monomer sequences of both DTMSS and styrene in the copolymer chain were very close to random. Plots of the total conversion versus the normalized concentrations of the monomers (**Figure 2b)** show the incorporation behavior. It is clear that both DTMSS and styrene nearly follow the classical profile of random incorporation of monomers that is shown as the dotted line in **Figure 2b**.

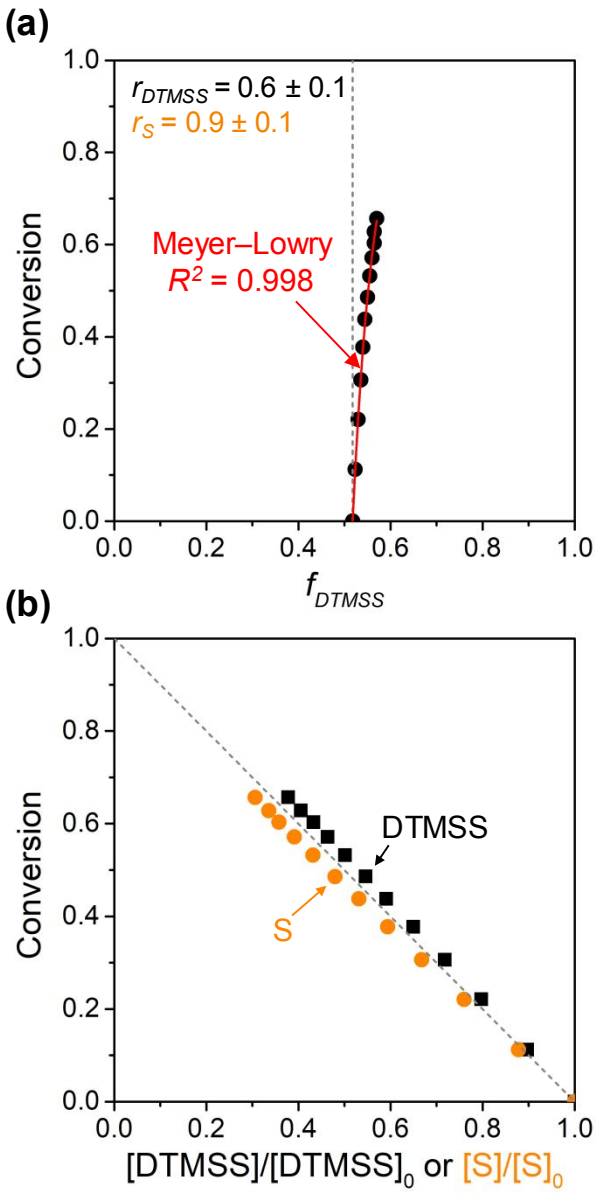

Figure 2. Overall conversion of a copolymerization of DTMSS and styrene (S) was measured every hour for 11 h and expressed as a function of (a) feed composition of DTMSS (f_{DTMSS}) and (b) normalized concentration of monomer ([DTMSS]/[DTMSS]$_0$ or [S]/[S]$_0$), respectively. Reactivity ratios of DTMSS and S were extracted from Meyer–Lowry model (red line in (a)).

The copolymerization of DtBS and styrene was carried out in the same way to determine their reactivity ratios. The results of the copolymerization kinetics study by ^{1}H NMR spectroscopy are shown in **Figure S7**. The copolymerization kinetics data for DtBS and styrene are summarized

in **Table S3**. As shown in **Figure S8**, the reactivity ratios of DtBS and styrene were determined to be $r_{DtBS} = 0.3 \pm 0.1$ and $r_S = 0.7 \pm 0.1$, respectively. For the purpose of comparison, an integrated nonterminal model for copolymerization developed by Beckingham *et al*. (BSL) was also used to extract the reactivity ratios (**Figure S9**).[39] Since there was a difference in the reactivity ratios between the nonterminal BSL model and the terminal Meyer–Lowry model, the terminal model of the copolymerization took precedence.[38] The incorporation of DtBS and styrene monomers into the copolymer was also very close to random.

Fortunately, it was not necessary to control monomer addition rates in order to achieve random copolymer sequences for styrene and the 3,5-disubstituted styrenes (PDTMSS or PDtBS). When the total conversion is kept relatively low (< 40%), the statistical copolymer obtained is sufficiently random to minimize the effect of composition gradients on the relationship between the T_g and the composition of the copolymer.

Six different copolymers of styrene (S) with varying monomer compositions of DTMSS and DtBS were synthesized by free radical copolymerization to conversion below 40%. The molecular weight (M_n) and the dispersity ($Đ$) of poly(3,5-di(trimethylsilyl)styrene-*co*-styrene) (P(DTMSS-*co*-S)) and poly(3,5-di-*tert*-butylstyrene-*co*-styrene) (P(DtBS-*co*-S)) were characterized by size exclusion chromatography, and the results are shown in **Figure S10** and **Table S4**. ^{1}H NMR spectroscopy was used to determine the P(DTMSS-*co*-S) copolymer composition, which was plotted against the monomer feed ratio as shown in **Figure S11**. The solid line in the plot shows the random copolymerization. The experimental data are all very close to the line, indicating the random nature of the copolymerization. The P(DtBS-*co*-S) copolymer composition based on DtBS (f_{DtBS}) cannot be determined directly by ^{1}H NMR due to peak overlap. However, the actual f_{DtBS} must be very close to the feed f_{DtBS}, which is the monomer feed ratio

based on DtBS. To be consistent, the following calculations were all based on the monomer feed f_{DTMSS} or the feed f_{DtBS}.

The T_gs of all of the copolymers were determined by DSC as shown in **Figure S12**. The P(DTMSS-*co*-S) and P(DtBS-*co*-S) copolymers showed very similar behavior. The T_g, which shows as an endothermic stepwise change of heat flow, is clearly evident for copolymers with 3,5-disubstituted styrene compositions below 90 mol%. As expected, the T_g shifts toward higher temperature with increasing molar fractions of 3,5-disubstituted styrene (DTMSS or DtBS) in the copolymer. The heat flow change at T_g gets smaller with increasing 3,5-disubstituted styrene incorporation. When the molar fraction of 3,5-disubstituted styrene is above 90 mol %, the heat flow is so small that it is very hard to assign a T_g region. No evidence of T_g is apparent for the DTMSSS or DtBS homopolymer. It should be noted that the copolymer samples containing > 90 mol% of 3,5-disubstituted styrene for the DSC test are still free-flowing powders after three heating (to 180 °C) and cooling cycles (**Figure S12d**), while the copolymer samples containing < 90 mol% of 3,5-disubstituted styrene fuse and appear glassy after the DSC test (**Figure S12c**).

The T_g can be defined as the midpoint in the range of the glass transition region.[40] The plots of T_g versus the mole fraction of 3,5-disubstituted styrene (DTMSS or DtBS) in the statistical copolymers are shown in **Figure 3**. Two experimental fitting models, the Fox model[41] and the Gordon–Taylor (GT) model,[28] were used to fit these data in an attempt to determine the T_g of the 3,5-disubstituted styrene homopolymer (PDTMSS or PDtBS). These two models were developed to determine the T_g of a binary polymer blend based on knowledge of the T_g of each polymer. However, the analyses were found to be applicable to evaluation of the T_g of a statistical copolymer as well as a blend.[42] For a polymer blend composed of homopolymers A and B, the Fox model for

a binary polymer blend made of homopolymers A and B is given by **eq 10**. The assumption is that individual homopolymers contribute equally to the properties of the blend.

$$\frac{1}{T_g} = \frac{x_A}{T_{g,A}} + \frac{1-x_A}{T_{g,B}} \tag{10}$$

Here x_A is the mass fraction of homopolymer A in the blend, $T_{g,A}$ and $T_{g,B}$ are T_gs of homopolymers A and B, respectively. The GT model assumes unequal contributions of the individual homopolymers and an additive rule based on the volume of the blend and a fitting parameter k_{GT} is employed as shown in **eq 11**:

$$T_g = \frac{x_A T_{g,A} + k_{GT}(1-x_A)T_{g,B}}{x_A + k_{GT}(1-x_A)} \tag{11}$$

where $T_{g,B}$ is higher than $T_{g,A}$, x_A is the mass fraction of homopolymer A in the blend.

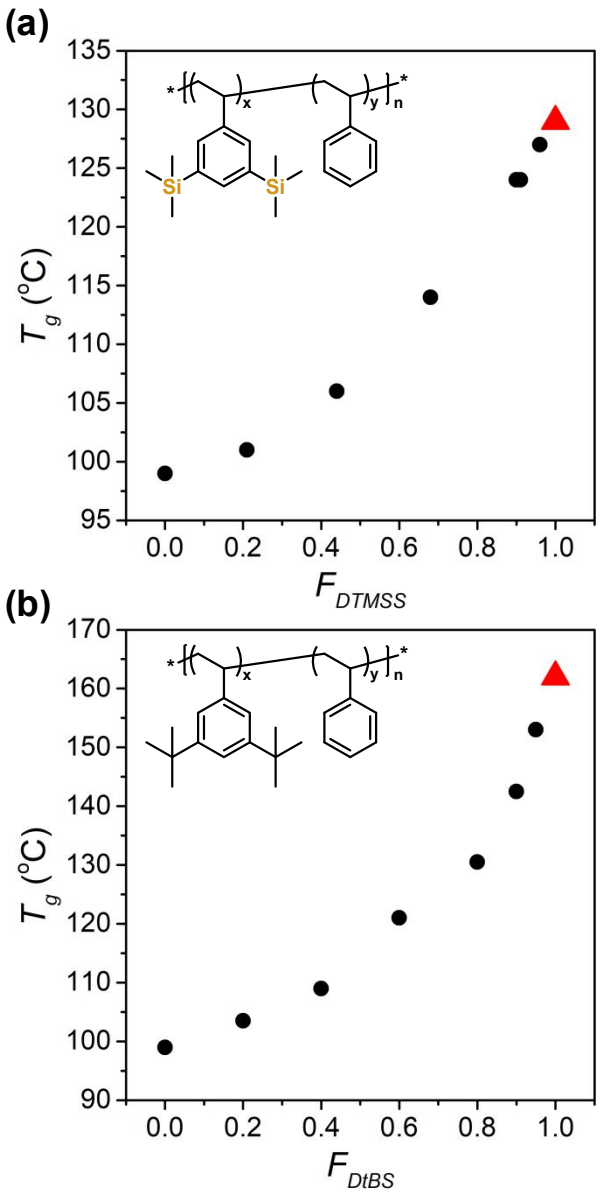

Figure 3. Dependence of T_gs of styrene-based statistical copolymers on 3,5-disubstituted styrene compositions: (a) P(DTMSS-*co*-S) and (b) P(DtBS-*co*-S), respectively. Red triangle markers indicate the extrapolated values of T_g of (a) PDTMSS and (b) PDtBS homopolymers by Gordon–Taylor model.[28]

These two models were used to fit the data plotted in **Figure 3** in order to extrapolate the T_gs of PDTMSS and PDtBS homopolymers (**Figure S13**). The Fox model did not fit the data well showing an R^2 of ~0.83 for both homopolymers. On the other hand, the GT model fit very well

with an R^2 of > 0.99, and it estimated the T_gs of PDTMSS and PDtBS to be 130 °C and 161 °C, respectively. The fitting parameter k_{GT} as well as the T_gs of PDTMSS and PDtBS calculated by both models are shown in **Table S5**. These data, the DMA, and the BDS measurements all point to some sort of transition in the range of 130–170 °C, but not a conventional glass transition because both the PDTMSS and the PDtBS homopolymers remain powdery after being heated to greater than 200 °C.

Incorporation of a tertiary substituted group into the polymer can significantly increase T_g compared to unmodified polymers without this bulky group because the steric hindrance of the bulky group reduces the mobility of the polymer backbone.[22,43–46] In addition, it was also found that the T_g increase for ortho substitution is much greater than the T_g increase for para substitution, which may be interpreted to mean that the steric hindrance at the ortho position creates a greater restriction on backbone motion because the ortho position is closer to the backbone. Even though the two substituent groups are at meta positions in PDTMSS or PDtBS, they are very bulky and also quite close to the polymer backbone. These two bulky groups must reduce relative backbone motion, which would explain why PDTMSS and PDtBS do not show any glass transition before onset of decomposition.

Conclusions

The fact that a PDTMSS-*b*-PMDOS diblock copolymer remained as a powder after being annealed at very high temperature inspired the determination of the T_gs of the PDTMSS homopolymer and its analog, the PDtBS homopolymer, by a variety of characterization techniques. PDTMSS and PDtBS show very similar thermal properties. No classical glass transition was observed in the DSC measurement for either polymer nor did they show any signs of changes in reflectivity in a melting point apparatus. The T_gs determined by *in-situ* ellipsometry, broadband dielectric spectroscopy, or extrapolation from the T_gs of copolymers with different compositions were all inconsistent with the results from both the DSC and measurements using the melting point apparatus. PDTMSS and PDtBS remain powdery before and after several heating cycles above the predicted or measured transitions. These observations are consistent with the existence of secondary relaxations but not consistent with a classical glass transition. It is clear that monomers made by substituting hydrogens on styrene with groups containing tertiary carbons or trisubstituted silicon at the 3 and 5 position can be used to produce soluble polymers with unusual thermal properties. These properties may be of interest to those designing membranes or plastics for use at temperatures well above the glass transition of PS.

ASSOCIATED CONTENT

Supporting Information.

The Supporting Information is available free of charge.

Additional experimental data (PDF)

AUTHOR INFORMATION

Corresponding Authors

*Email: willson@che.utexas.edu (C.G.W.)

Author Contributions

†(J.H.K. and Q.Z.) These authors contributed equally.

Notes

These authors declare no competing financial interest.

ACKNOWLEDGMENT

The authors are grateful for financial support from The Rashid Engineering Regents Chair, The Welch Foundation (grant # F-1830), Nissan Chemical Company, and Kwanjeong Educational Foundation. EUM and JRS acknowledge financial support from National Science Foundation through DMR-1508394.

REFERENCES

(1) Bates, F. S.; Fredrickson, G. H. Block Copolymers-Designer Soft Materials. *Phys. Today* **2000**, *52*, 32.

(2) Azarnouche, L.; Sirard, S. M.; Durand, W. J.; Blachut, G.; Gurer, E.; Hymes, D. J.; Ellison, C. J.; Willson, C. G.; Graves, D. B. Plasma and Photon Interactions with Organosilicon Polymers for Directed Self-Assembly Patterning Applications. *J. Vac. Sci. Technol. B, Nanotechnol. Microelectron. Mater. Process. Meas. Phenom.* **2016**, *34*, 061602.

(3) Maher, M. J.; Mori, K.; Sirard, S. M.; Dinhobl, A. M.; Bates, C. M.; Gurer, E.; Blachut, G.; Lane, A. P.; Durand, W. J.; Carlson, M. C. Pattern Transfer of Sub-10 Nm Features via Tin-Containing Block Copolymers. *ACS Macro Lett.* **2016**, *5*, 391–395.

(4) Son, J. G.; Gotrik, K. W.; Ross, C. A. High-Aspect-Ratio Perpendicular Orientation of PS-b-PDMS Thin Films under Solvent Annealing. *ACS Macro Lett.* **2012**, *1*, 1279–1284.

(5) Jung, Y. S.; Ross, C. A. Orientation-Controlled Self-Assembled Nanolithography Using a Polystyrene−Polydimethylsiloxane Block Copolymer. *Nano Lett.* **2007**, *7*, 2046–2050.

(6) Bai, W.; Hannon, A. F.; Gotrik, K. W.; Choi, H. K.; Aissou, K.; Liontos, G.; Ntetsikas, K.; Alexander-Katz, A.; Avgeropoulos, A.; Ross, C. A. Thin Film Morphologies of Bulk-Gyroid Polystyrene-Block-Polydimethylsiloxane under Solvent Vapor Annealing. *Macromolecules* **2014**, *47*, 6000–6008.

(7) Lutz, J. F.; Lehn, J. M.; Meijer, E. W.; Matyjaszewski, K. From Precision Polymers to Complex Materials and Systems. *Nat. Rev. Mater.* **2016**, *1*.

(8) Pitet, L. M.; Wuister, S. F.; Peeters, E.; Kramer, E. J.; Hawker, C. J.; Meijer, E. W. Well-Organized Dense Arrays of Nanodomains in Thin Films of Poly(Dimethylsiloxane)-b-Poly(Lactide) Diblock Copolymers. *Macromolecules* **2013**, *46*, 8289–8295.

(9) Inoue, H.; Matsumoto, A.; Matsukawa, K.; Ueda, A.; Nagai, S. Surface Characteristics of Polydimethylsiloxane—Poly(Methyl Methacrylate) Block Copolymers and Their PMMA Blends. *J. Appl. Polym. Sci.* **1990**, *41*, 1815–1829.

(10) Rodwogin, M. D.; Spanjers, C. S.; Leighton, C.; Hillmyer, M. A. Polylactide - Poly(Dimethylsiloxane) - Polylactide Triblock Copolymers as Multifunctional Materials for Nanolithographic Applications. *ACS Nano* **2010**, *4*, 725–732.

(11) Bates, C. M.; Seshimo, T.; Maher, M. J.; Durand, W. J.; Cushen, J. D.; Dean, L. M.; Blachut, G.; Ellison, C. J.; Willson, C. G. Polarity-Switching Top Coats Enable Orientation of Sub-10-Nm Block Copolymer Domains. *Science (80-.).* **2012**, *338*, 775–779.

(12) Seshimo, T.; Bates, C. M.; Dean, L. M.; Cushen, J. D.; Durand, W. J.; Maher, M. J.; Ellison, C. J.; Willson, C. G. Block Copolymer Orientation Control Using a Top-Coat Surface Treatment. *J. Photopolym. Sci. Technol.* **2012**, *25*, 125–130.

(13) Maher, M. J.; Bates, C. M.; Blachut, G.; Sirard, S.; Self, J. L.; Carlson, M. C.; Dean, L. M.; Cushen, J. D.; Durand, W. J.; Hayes, C. O.; et al. Interfacial Design for Block Copolymer Thin Films. *Chem. Mater.* **2014**, *26*, 1471–1479.

(14) Durand, W. J.; Blachut, G.; Maher, M. J.; Sirard, S.; Tein, S.; Carlson, M. C.; Asano, Y.; Zhou, S. X.; Lane, A. P.; Bates, C. M.; et al. Design of High-χ Block Copolymers for Lithography. *J. Polym. Sci. Part A Polym. Chem.* **2015**, *53*, 344–352.

(15) Maher, M. J.; Rettner, C. T.; Bates, C. M.; Blachut, G.; Carlson, M. C.; Durand, W. J.; Ellison, C. J.; Sanders, D. P.; Cheng, J. Y.; Willson, C. G. Directed Self-Assembly of Silicon-Containing Block Copolymer Thin Films. *ACS Appl. Mater. Interfaces* **2015**, *7*, 3323–3328.

(16) Blachut, G.; Sirard, S. M.; Maher, M. J.; Asano, Y.; Someya, Y.; Lane, A. P.; Durand, W. J.; Bates, C. M.; Dinhobl, A. M.; Gronheid, R.; et al. A Hybrid Chemo-/Grapho-Epitaxial Alignment Strategy for Defect Reduction in Sub-10 Nm Directed Self-Assembly of Silicon-Containing Block Copolymers. *Chem. Mater.* **2016**, *28*, 8951–8961.

(17) Someya, Y.; Asano, Y.; Maher, M. J.; Blachut, G.; Lane, A. P.; Sirard, S.; Ellison, C. J.; Willson, C. G. Synthesis and Characterization of Si-Containing Block Co-Polymers with Resolution beyond 10 Nm. *J. Photopolym. Sci. Technol.* **2016**, *29*, 701–704.

(18) Cushen, J. D.; Bates, C. M.; Rausch, E. L.; Dean, L. M.; Zhou, S. X.; Willson, C. G.; Ellison, C. J. Thin Film Self-Assembly of Poly(Trimethylsilylstyrene-b-d, l-Lactide) with Sub-10 Nm Domains. *Macromolecules* **2012**, *45*, 8722–8728.

(19) Bates, C. M.; Pantoja, M. A. B.; Strahan, J. R.; Dean, L. M.; Mueller, B. K.; Ellison, C. J.; Nealey, P. F.; Willson, C. G. Synthesis and Thin-film Orientation of Poly (Styrene-block-trimethylsilylisoprene). *J. Polym. Sci. Part A Polym. Chem.* **2013**, *51*, 290–297.

(20) Lane, A. P.; Yang, X.; Maher, M. J.; Blachut, G.; Asano, Y.; Someya, Y.; Mallavarapu, A.; Sirard, S. M.; Ellison, C. J.; Willson, C. G. Directed Self-Assembly and Pattern Transfer of Five Nanometer Block Copolymer Lamellae. *ACS Nano* **2017**, *11*, 7656–7665.

(21) Sunday, D. F.; Maher, M. J.; Hannon, A. F.; Liman, C. D.; Tein, S.; Blachut, G.; Asano, Y.; Ellison, C. J.; Willson, C. G.; Kline, R. J. Characterizing the Interface Scaling of High χ Block Copolymers near the Order–Disorder Transition. *Macromolecules* **2017**, *51*, 173–180.

(22) Kowalewska, A. Hybrid Polymeric Systems Bearing Bulky Derivatives of Tris (Trimethylsilyl) Methane. *RSC Adv.* **2014**, *4*, 9622–9631.

(23) Safa, K. D.; Babazadeh, M.; Namazi, H.; Mahkam, M.; Asadi, M. G. Synthesis and Characterization of New Polymer Systems Containing Very Bulky Tris(Trimethylsilyl)Methyl Substituents as Side Chains. *Eur. Polym. J.* **2004**, *40*, 459–466.

(24) Safa, K. D.; Babazadeh, M. Synthesis and Characterization of 4-Chloromethylstyrene Polymers Containing Bulky Organosilicon Groups. *e-Polymers* **2004**, *4*.

(25) Dalnoki-Veress, K.; Forrest, J. A.; Murray, C.; Gigault, C.; Dutcher, J. R. Molecular Weight Dependence of Reductions in the Glass Transition Temperature of Thin, Freely Standing Polymer Films. *Phys. Rev. E* **2001**, *63*, 31801.

(26) Ellison, C. J.; Torkelson, J. M. The Distribution of Glass-Transition Temperatures in Nanoscopically Confined Glass Formers. *Nat. Mater.* **2003**, *2*, 695–700.

(27) Kawana, S.; Jones, R. A. L. Character of the Glass Transition in Thin Supported Polymer Films. *Phys. Rev. E* **2001**, *63*, 021501.

(28) Gordon, M.; Taylor, J. S. Ideal Copolymers and the Second-Order Transitions of Synthetic Rubbers. i. Non-Crystalline Copolymers. *J. Appl. Chem.* **1952**, *2*, 493–500.

(29) Mapesa, E. U.; Tress, M.; Schulz, G.; Huth, H.; Schick, C.; Reiche, M.; Kremer, F. Segmental and Chain Dynamics in Nanometric Layers of Poly(Cis-1,4-Isoprene) as Studied by Broadband Dielectric Spectroscopy and Temperature-Modulated Calorimetry. *Soft Matter* **2013**, *9*, 10592–10598.

(30) Heres, M.; Cosby, T.; Mapesa, E. U.; Sangoro, J. Probing Nanoscale Ion Dynamics in Ultrathin Films of Polymerized Ionic Liquids by Broadband Dielectric Spectroscopy. *ACS Macro Lett.* **2016**, *5*, 1065–1069.

(31) Serghei, A.; Kremer, F. Broadband Dielectric Studies on the Interfacial Dynamics Enabled by Use of Nanostructured Electrodes. *Rev. Sci. Instrum.* **2008**, *79*, 26101.

(32) Havriliak, S.; Negami, S. A Complex Plane Representation of Dielectric and Mechanical Relaxation Processes in Some Polymers. *Polymer (Guildf).* **1967**, *8*, 161–210.

(33) Wübbenhorst, M.; van Turnhout, J. Analysis of Complex Dielectric Spectra. I. One-Dimensional Derivative Techniques and Three-Dimensional Modelling. *J. Non. Cryst. Solids* **2002**, *305*, 40–49.

(34) Ryzhov, V. A. Relationship Between the Molecular Dynamics of Polystyrene and Its Modifications and Parameters of Poley Absorption in Far-Infrared Spectra. *J. Macromol. Sci. Part B* **2013**, *52*, 1662–1673.

(35) Kremer, F.; Schoenhals, A. In *Broadband Dielectric Spectroscopy*; Springer: Berlin, 2003.

(36) Meyer, V. E.; Lowry, G. G. Integral and Differential Binary Copolymerization Equations. *J. Polym. Sci. Part A Gen. Pap.* **1965**, *3*, 2843–2851.

(37) Chwatko, M.; Lynd, N. A. Statistical Copolymerization of Epoxides and Lactones to High Molecular Weight. *Macromolecules* **2017**, *50*, 2714–2723.

(38) Lynd, N. A.; Ferrier, R. C.; Beckingham, B. S. Recommendation for Accurate Experimental Determination of Reactivity Ratios in Chain Copolymerization. *Macromolecules* **2019**, *52*, 2277–2285.

(39) Beckingham, B. S.; Sanoja, G. E.; Lynd, N. A. Simple and Accurate Determination of Reactivity Ratios Using a Nonterminal Model of Chain Copolymerization. *Macromolecules* **2015**, *48*, 6922–6930.

(40) Kalichevsky, M. T.; Jaroszkiewicz, E. M.; Ablett, S.; Blanshard, J. M. V.; Lillford, P. J. The Glass Transition of Amylopectin Measured by DSC, DMTA and NMR. *Carbohydr. Polym.* **1992**, *18*, 77–88.

(41) Fox, T. G. Influence of Diluent and of Copolymer Composition on the Glass Temperature of a Polymer System. *Bull. Am. Phys. Soc.* **1956**, *1*, 123.

(42) Brostow, W.; Chiu, R.; Kalogeras, I. M.; Vassilikou-Dova, A. Prediction of Glass Transition Temperatures: Binary Blends and Copolymers. *Mater. Lett.* **2008**, *62*, 3152–3155.

(43) Camelio, P.; Lazzeri, V.; Waegell, B.; Cypcar, C.; Mathias, L. J. Glass Transition Temperature Calculations for Styrene Derivatives Using the Energy, Volume, and Mass Model. *Macromolecules* **1998**, *31*, 2305–2311.

(44) Chaumont, P.; Beinert, G.; Herz, J.; Rempp, P. Synthesis and Properties of Poly (2, 4, 6-trimethylstyrene). *Die Makromol. Chemie Macromol. Chem. Phys.* **1979**, *180*, 2061–2071.

(45) Safa, K. D.; Babazadeh, M.; Namazi, H.; Mahkam, M.; Asadi, M. G. Synthesis and Characterization of New Polymer Systems Containing Very Bulky Tris (Trimethylsilyl) Methyl Substituents as Side Chains. *Eur. Polym. J.* **2004**, *40*, 459–466.

(46) Assadi, M. G.; Golipour, N. Synthesis and Characterization of New Monomer and Polymers of Hindered Silyl Styrene. *Des. monomers Polym.* **2007**, *10*, 79–89.

Table of Contents Graphic